CHAPTER 6

HIGHLY SENSITIVE BIOCHEMICAL SENSOR BASED ON PHOTONIC CRYSTAL RING RESONATOR

In this chapter a bio-chemical sensor is proposed based on photonic crystal ring resonator. The sensing characteristics of two types of ring resonator structures based on square and circular ring are studied and compared. The refractive index of coupling rods, inner ring rods and coupling as well as inner ring rods combined together are varied according to the sample which is to be sensed. Normalized transmission peaks at resonance condition are plotted against wavelength using finite difference time-domain (FDTD) technique. Plane wave expansion (PWE) method has been used to calculate the photonic bandgap of the proposed structures. It is found that both types of ring resonators have shown high sensitivity when the refractive index of sample is varied from 3.1 to 3.7 in steps of 0.2.

6.1 GENERAL

The optical devices based on photonic crystals (PCs) have generated a great attention due to their compact size, high speed of operations and large efficiency. PCs arranged in a periodic form have the property to limit the propagation of certain band of electromagnetic (EM) frequencies to pass through them. This range of frequency which is not allowed to pass through the PC structure is known as photonic bandgap. The photonic band gap plays a crucial role in realizing a large number of PC based optical devices. The optical devices which can be realized through PCs are optical switches, add-drop filters, multiplexers, de-multiplexers, power-splitters etc. One of the important areas of application of PC based

devices in recent times is in the bio-sensing region. A large number of bio-chemicals are present in the environment and it has always been a challenging task to detect and classify those chemicals in a faster and efficient manner. Researches have been conducted in order to make optical devices act as bio-sensors. Sensing has been performed through optical micro-ring resonators by [141, 142]. Works related to the detection of protein are done with the help of optical waveguides [93, 143]. E. Krioukov et al. [144] and E. Chow et al. [145] have shown the sensing characteristics of optical micro cavities in their work. Bio-sensors based on PCs have compact size, low cost of operations and are convenient to use. There can be done real-time monitoring of the signals generated through samples in PC based sensors.

In our work, we have presented an optical device called photonic crystal ring resonator (PCRR) [96] for bio-sensing applications. In 2014, Y. Chen et al. [91] have studied bio-sensing characteristics of PCRR in their work. They have shown variation of peaks, output from the PCRR structure with the change in the refractive index of sensing rods according to the biological sample. The sensing rods consist of inner ring rods present in the cavity as well as coupling rods which act as a transfer medium for EM wave from waveguide to cavity and vice-versa. In our work we have varied the refractive index of sensing rods as well as shape of the inner ring from circular to square in the PCRR structure. We have shown a highly sensitive bio-chemical sensor in our work, whose applications may vary from industrial to research sector.

6.2 STRUCTURE DESIGN

We have designed a 25 x 29 square lattice structure containing photonic crystal (PC) rods at the lattice points. Bandgap is calculated for this structure by adjusting the photonic

crystal rods radius and refractive index. The distance between two adjacent PC rods, known as lattice constant (a) is also varied for bandgap calculation. The refractive index, radius of the PC rods is set to be 4.15 and 0.165 µm respectively. Lattice constant is fixed at 0.615 µm in the designed structure. To calculate PBG of the designed structure, plane wave expansion (PWE) method was employed, by virtue of which we get two TE bandgaps as shown in Figure 6.1.

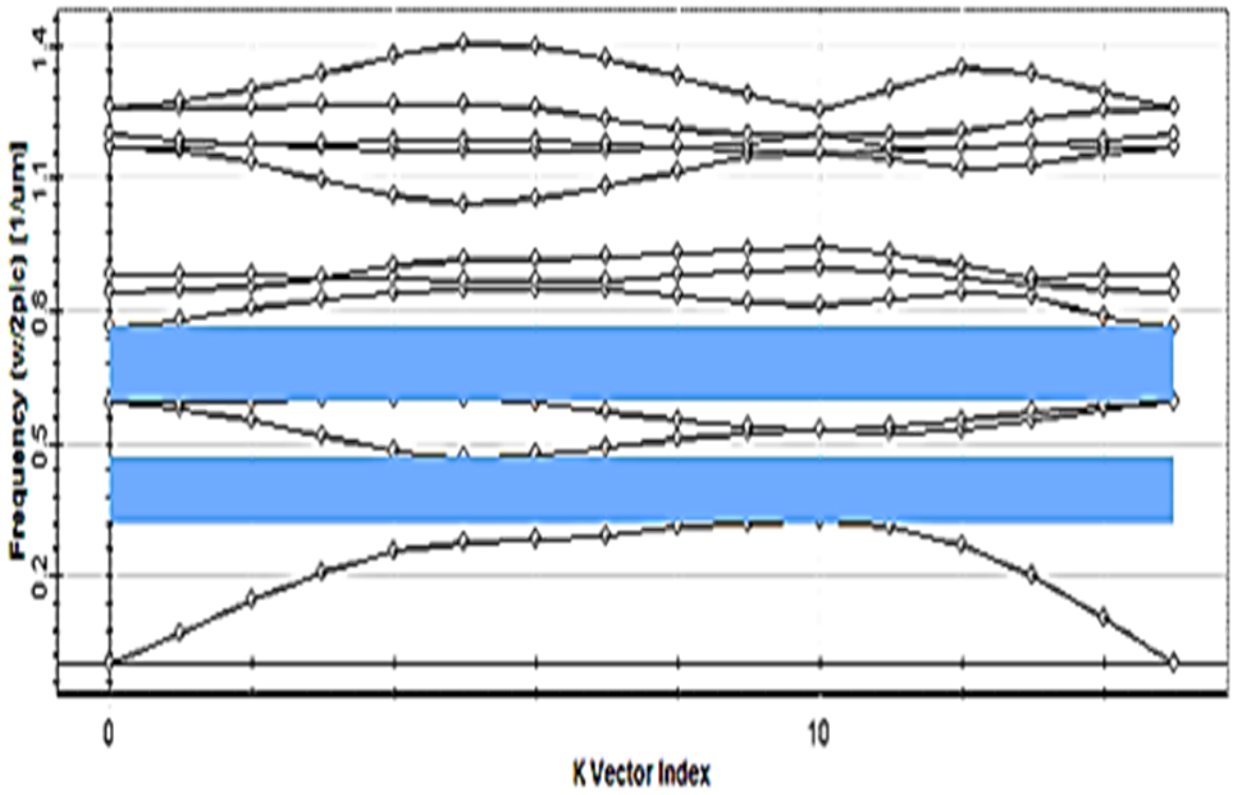

Figure 6.1 Band diagram of a 25 x 29 photonic crystal structure without the introduction of any defect.

Obtaining even one bandgap is enough for the source to be set at desired wavelength. We have considered the second bandgap starting from top in our simulation. Input

electromagnetic (EM) source is taken to be of Gaussian in nature with peak output at 1.55 µm. After finding out the PBG of the structure we made cavity in the center by eliminating few PC rods in a square region. Line waveguides are drawn to provide input to this cavity from the source placed on left direction and extract output in the right direction.

Two types of rings made of PCs are placed in the cavity to make two new structures respectively. Figure 6.2 shows a circular ring put in the cavity with the radius of ring fixed at 0.9 µm, which is the distance between the center of the cavity and any PC situated in that ring.

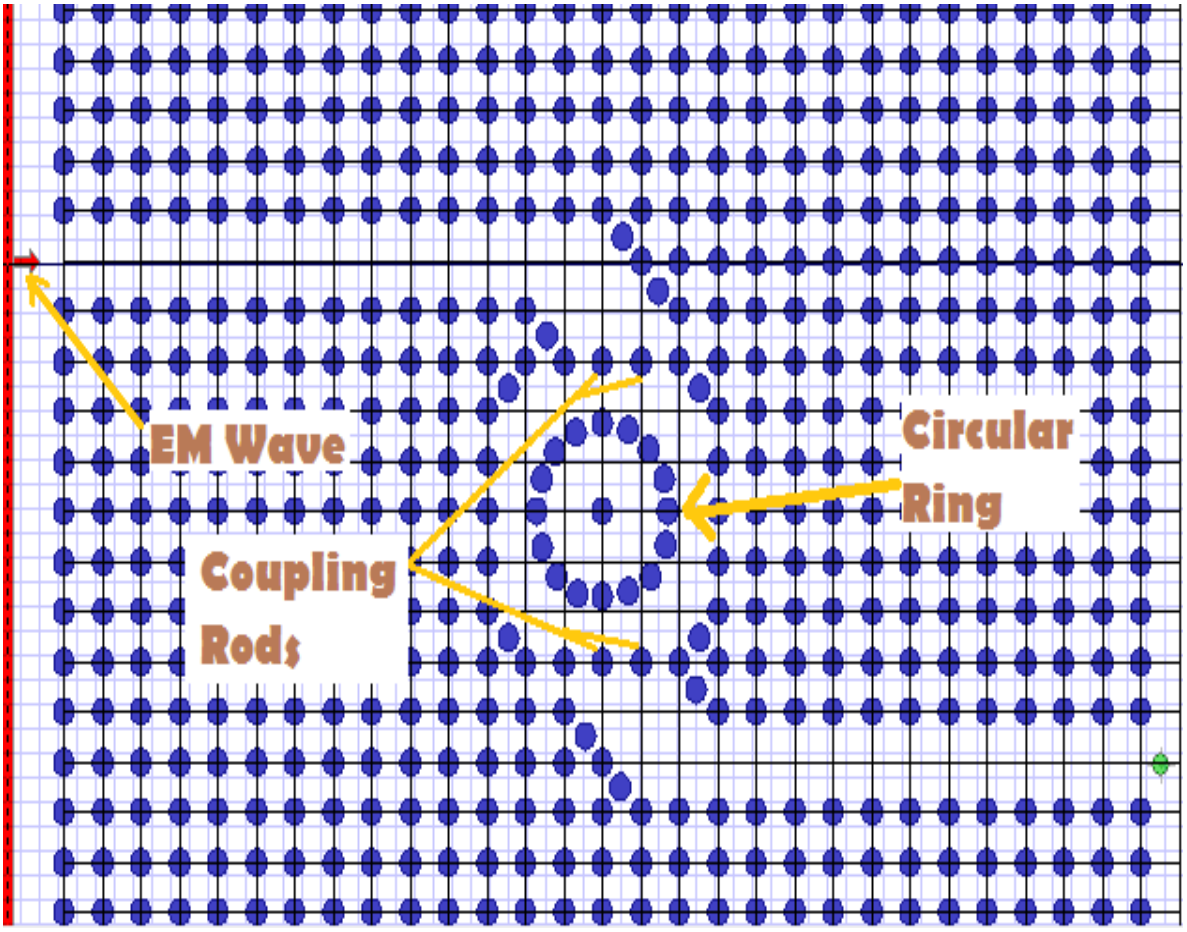

Figure 6.2 Layout of the PC based bio-chemical sensor with a circular ring.

For making a square ring to be placed in the cavity, we have first calculated the side of the square by finding its area. Firstly, the area of square is made equal to that of circular ring which is 2.54 μm^2 approx. Then applying the formula for finding the side of a square (a), we got a= 1.59 μm. The PC structure containing square ring is depicted in Figure 6.3.

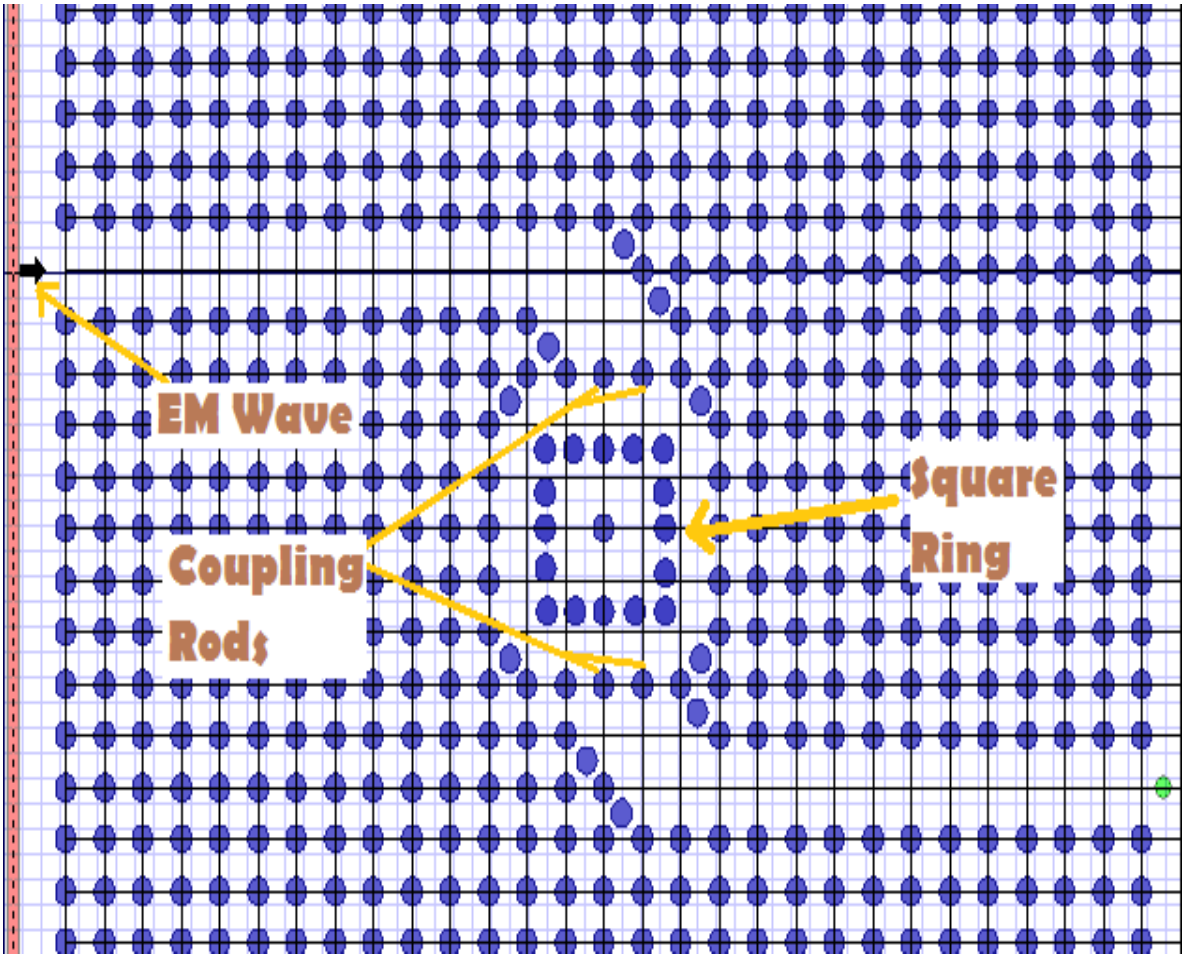

Figure 6.3 Layout of the PC based bio-chemical sensor with a square ring.

The areas of both circular as well as square rings are made equal so that the modes of the input EM wave at resonant condition have identical confinement areas. The only effect on the modes would be of the shape of the confinement region i.e., circular or square.

6.3 SIMULATION RESULTS AND DISCUSSION

We have simulated both the circular ring and square ring based PC structures for application in the bio-sensing regime. Finite-difference time domain technique [146] with perfectly matching layers (PMLs) is applied to calculate the transmission characteristics of the proposed sensor. At first, the refractive index of the coupling rods is only varied. The coupling rods are the PC's that are placed between the line waveguides and cavity. We have supposed the refractive index of the substance which is to be sensed equal to 2.2 and this refractive index is varied in steps of 0.02 until it reaches 2.28. Next, the refractive index of the inner ring (viz. circular or square) is varied again in the similar range as that for coupling rods. Finally the refractive index of both the inner rings and coupling rods is varied.

6.3.1 Variation of refractive index of coupling rods alone

For circular ring resonator we get the output resonant peaks as shown in Figure 6.4. There is observed a linear shift of the resonance center peaks on the wavelength scale corresponding to refractive index starting from 2.2 to 2.28.The peaks keep shifting right as the refractive index corresponding to them is being increased.

Figure 6.5 shows the output peaks of square ring photonic crystal structure. The resonance center peaks in this figure are also shifting linearly in the positive direction of wavelength as we keep increasing the refractive index of the coupling rods. Along the declining slope of the peaks in this figure, there is observed a constant relationship between transmission and wavelength. The constant behavior is observed around 50 % of the

transmission level for the first peak and around 30 % of the transmission level for the last peak corresponding to refractive index equal to 2.2 and 2.28 respectively.

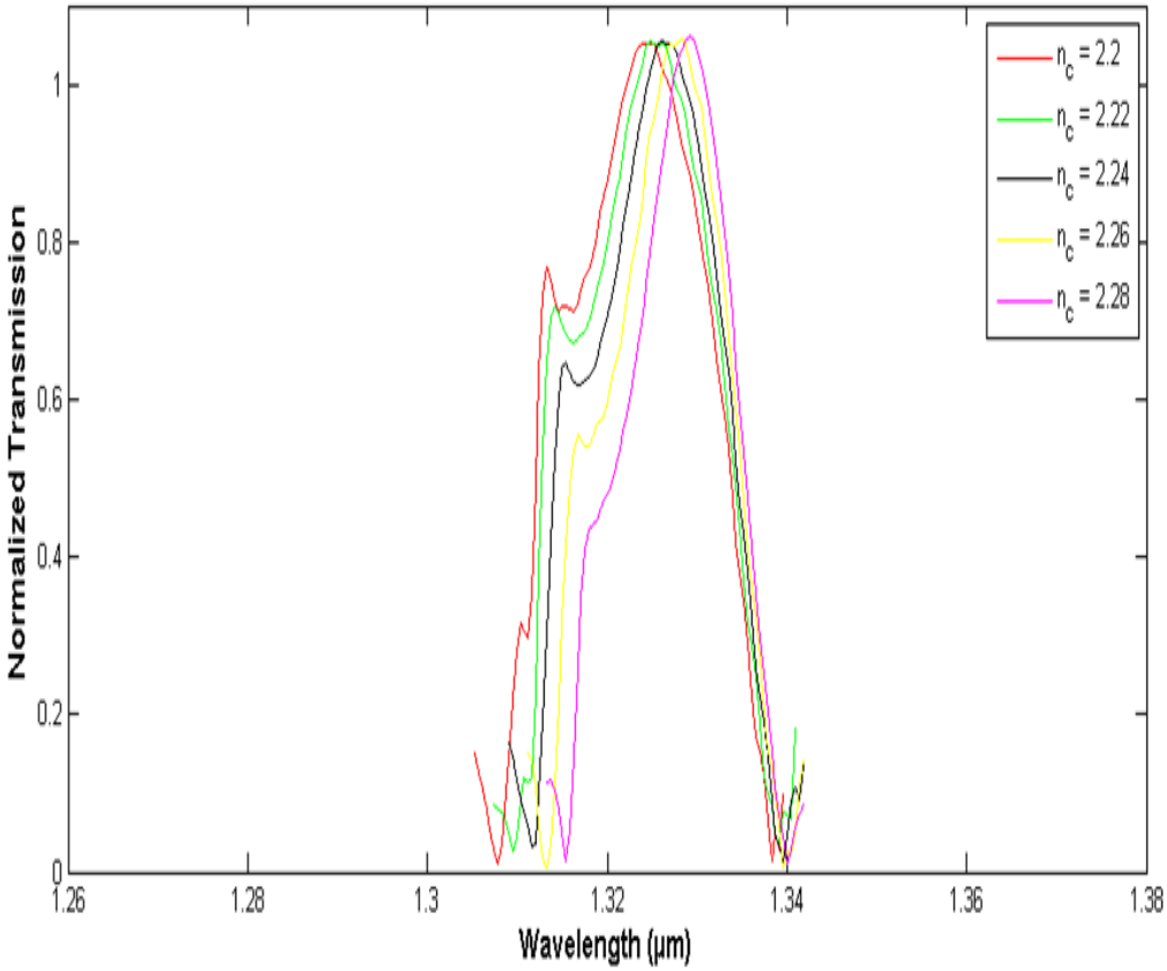

Figure 6.4 Normalized transmission spectra for the variation of refractive index of coupling rods according to the sample in circular ring structure.

We can say that we have got a transmission band around 50 % of the output level for peak corresponding refractive index equal to 2.2. This transmission band goes on decreasing to nearly 30 % for peak corresponding to refractive index equal to 2.28.

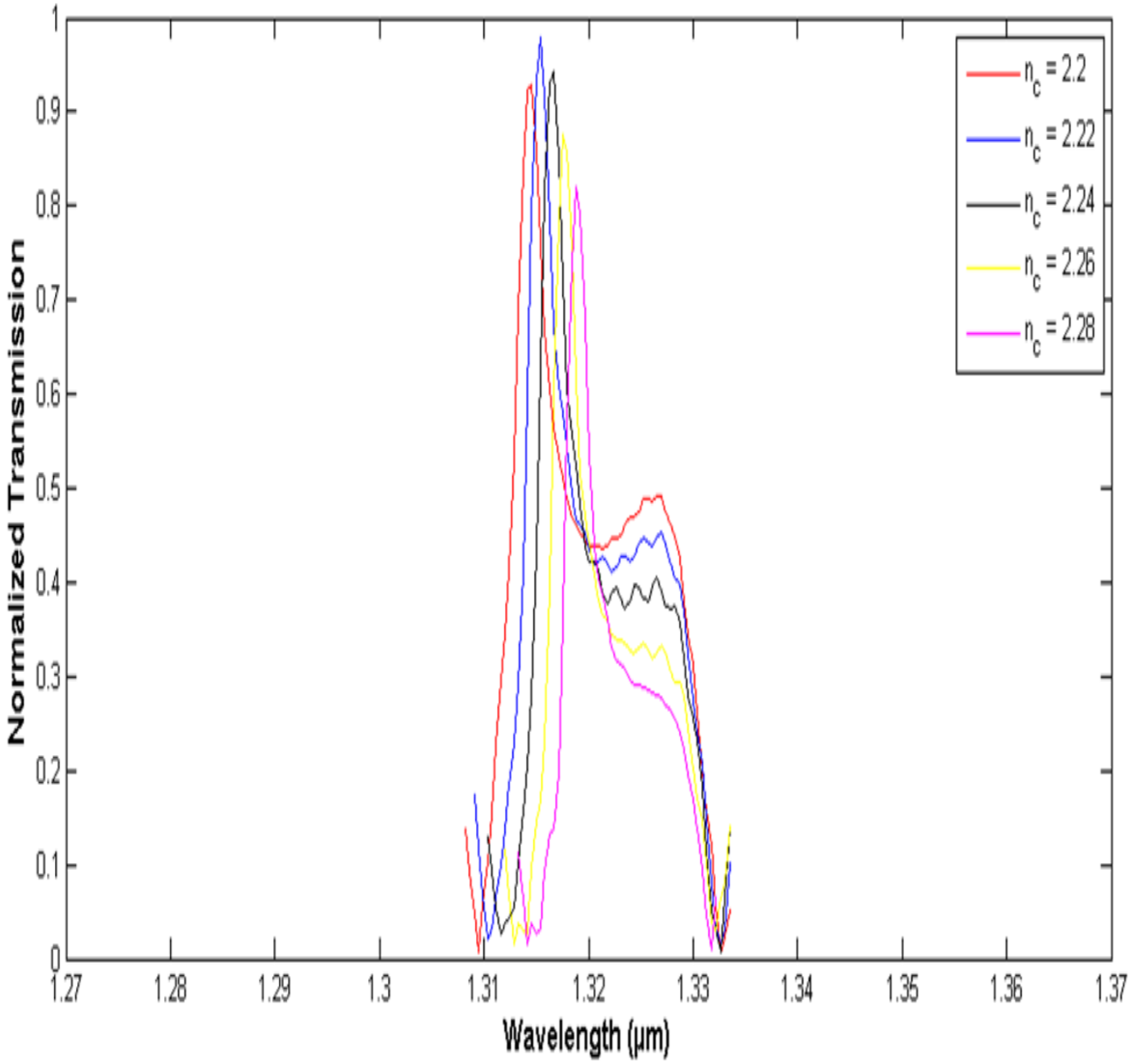

Figure 6.5 Normalized transmission spectra for the variation of refractive index of coupling rods according to the sample in the square ring structure.

6.3.2 Variation of refractive index of inner ring rods alone.

For circular ring structure as we vary the refractive index of the inner ring rods only, from 2.2 to 2.28, the output resonance center peaks shift from 1.403 to 1.417 μm in the positive direction on the wavelength scale as is visible in the Figure 6.6.

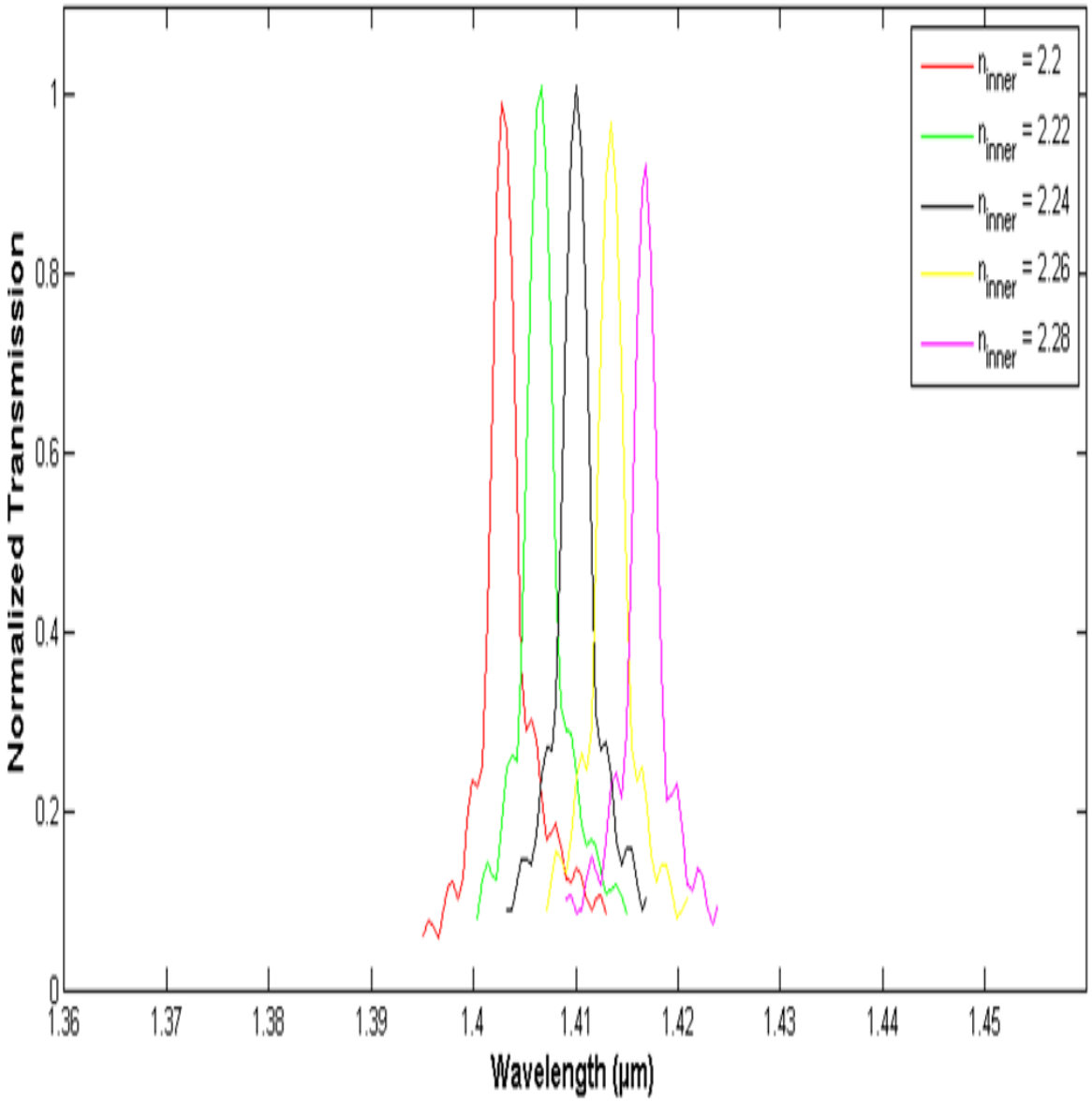

Figure 6.6 Normalized transmission spectra for the variation of refractive index of inner ring rods according to the sample in circular ring structure.

In case of square ring structure as we vary the refractive index of the inner ring rods, the output resonance center peaks shift from 1.445 to 1.458 μm again in the positive direction on the wavelength scale as can be seen in Figure 6.7. We can see that the first peak of the

square ring structure starts 42 nm ahead of the first peak of the circular ring structure in the right direction.

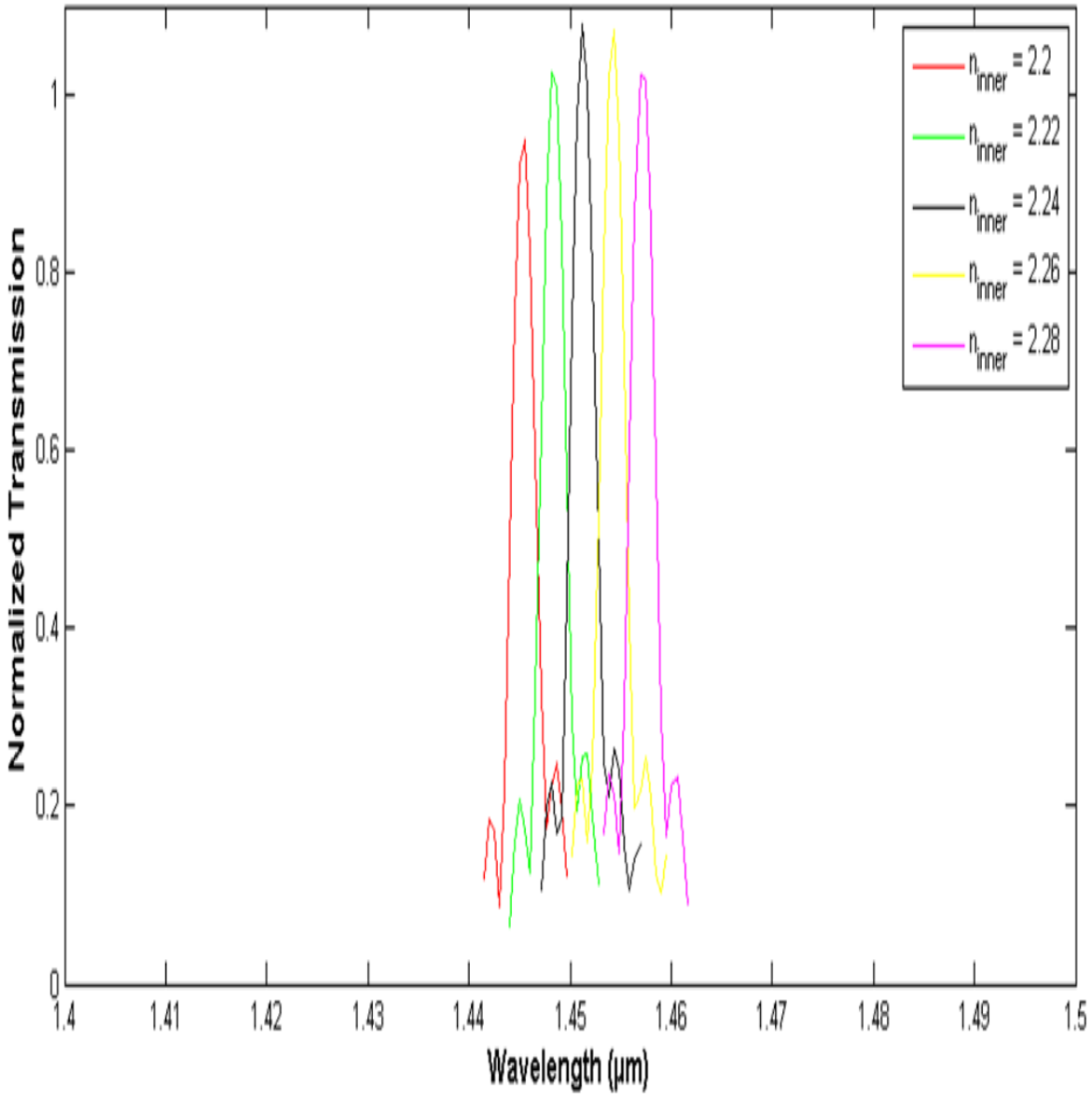

Figure 6.7 Normalized transmission spectra for the variation of refractive index of inner ring rods according to the sample in the square ring structure.

6.3.3 Variation of refractive index of both the coupling and inner ring rods.

Considering circular ring structure, as we vary refractive index of both the coupling and inner ring rods from 2.2 to 2.28, we see that the output resonant peak's width keeps getting narrower as we move in the increasing direction of wavelength as displayed in Figure 6.8.

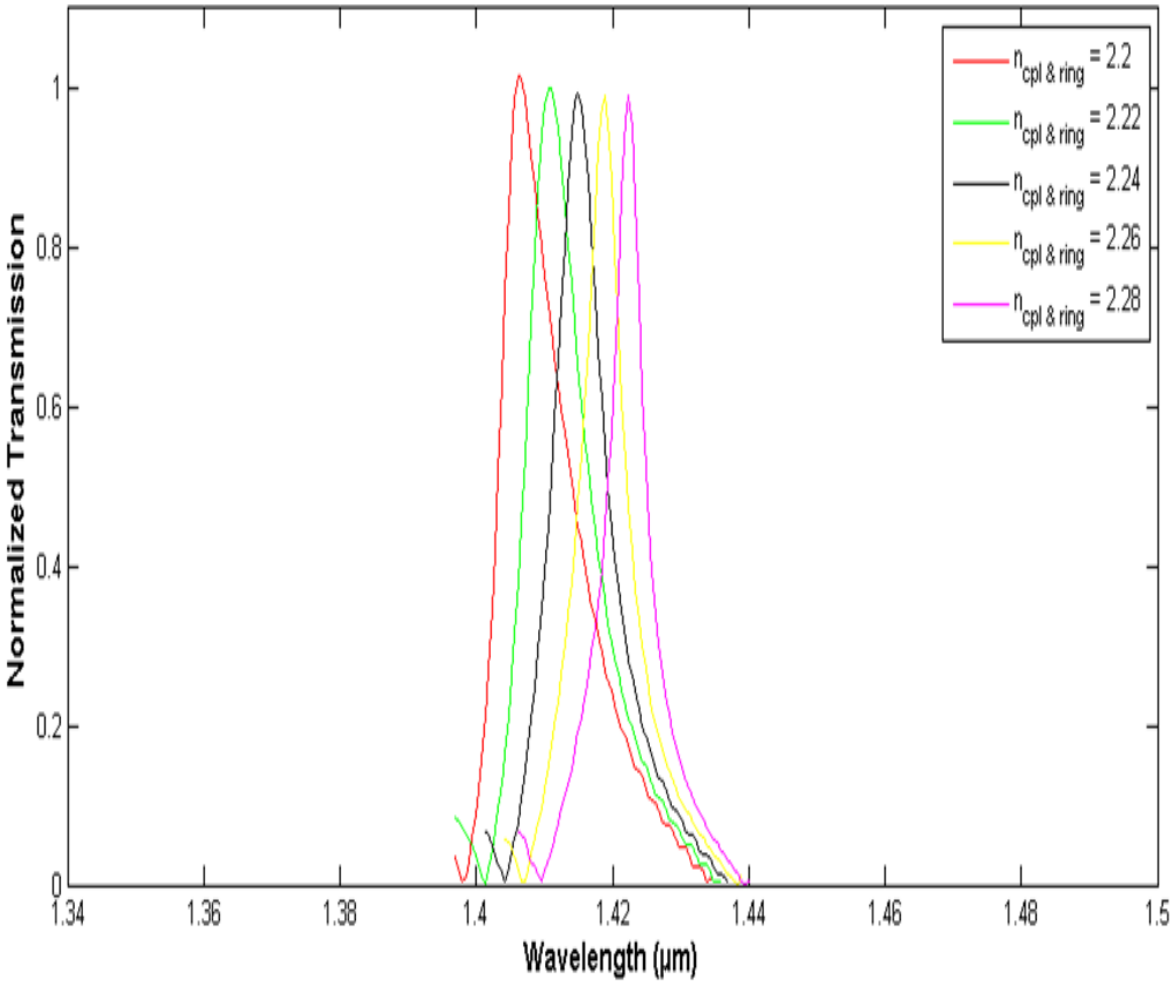

Figure 6.8 Normalized transmission spectra for the variation of refractive index of coupling rods as well as inner ring rods according to the sample in the circular ring structure.

The center of the resonant peak corresponding to refractive index 2.20 is at 1.406 μm and that of resonant peak corresponding to refractive index 2.28 is at 1.422 μm. The total shift

between the peaks is 16 nm. For the square ring structure also, as we vary the refractive index of both the coupling and inner ring rods, a decrease in the width of the output resonant peaks from left to right on the wavelength scale is observed (Figure 6.9).

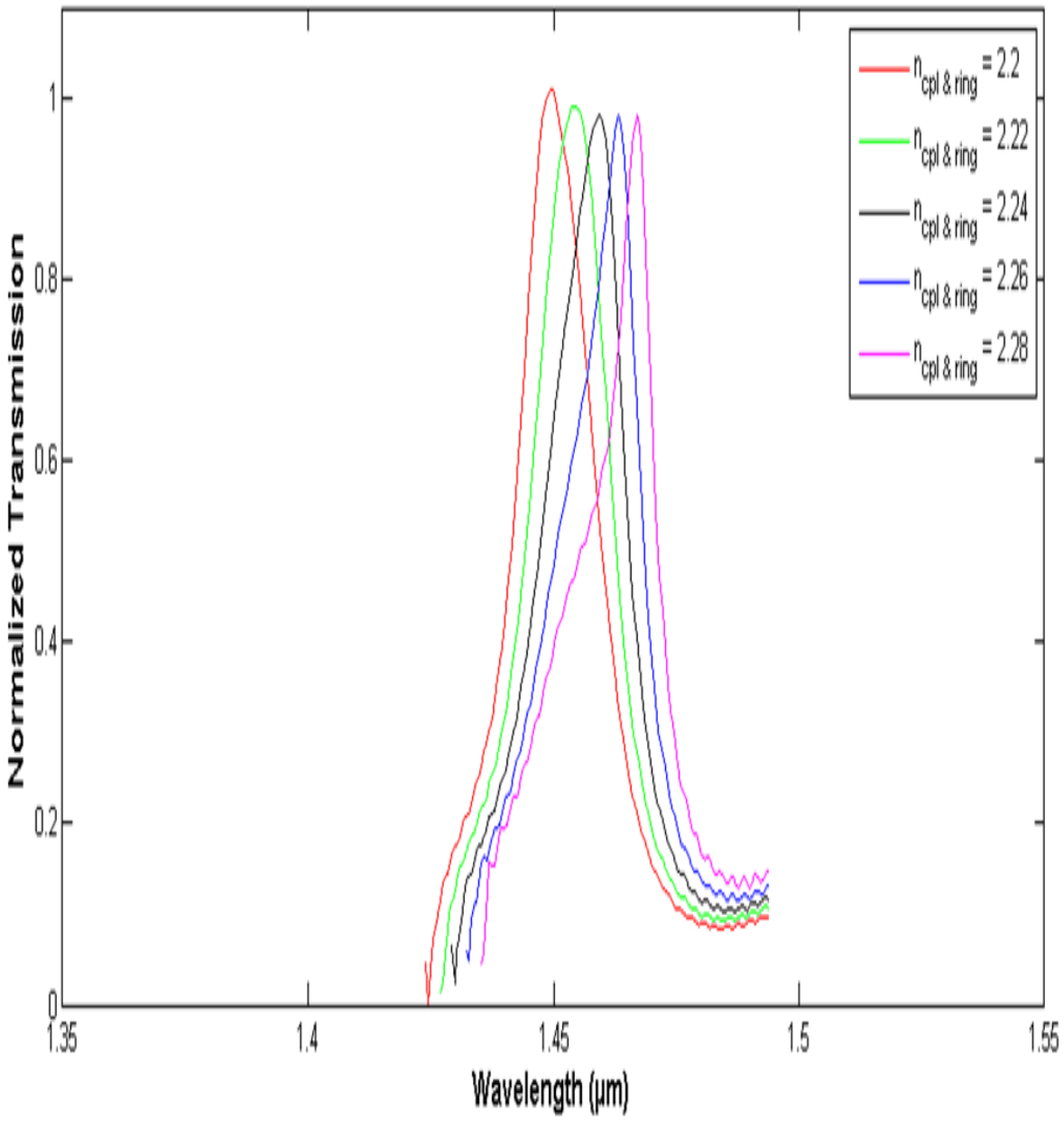

Figure 6.9 Normalized transmission spectra for the variation of refractive index of coupling rods as well as inner ring rods according to the sample in the square ring structure.

Here, the center of the resonant peak corresponding to refractive index 2.20 is at 1.449 µm and that of resonant peak corresponding to refractive index 2.28 is at 1.467 µm. The total shift between the peaks is 18 nm.

Figure 6.10 and Figure 6.11 show a relationship between the refractive index of samples and wavelength shift of the resonance center peaks of square ring and circular ring structure respectively.

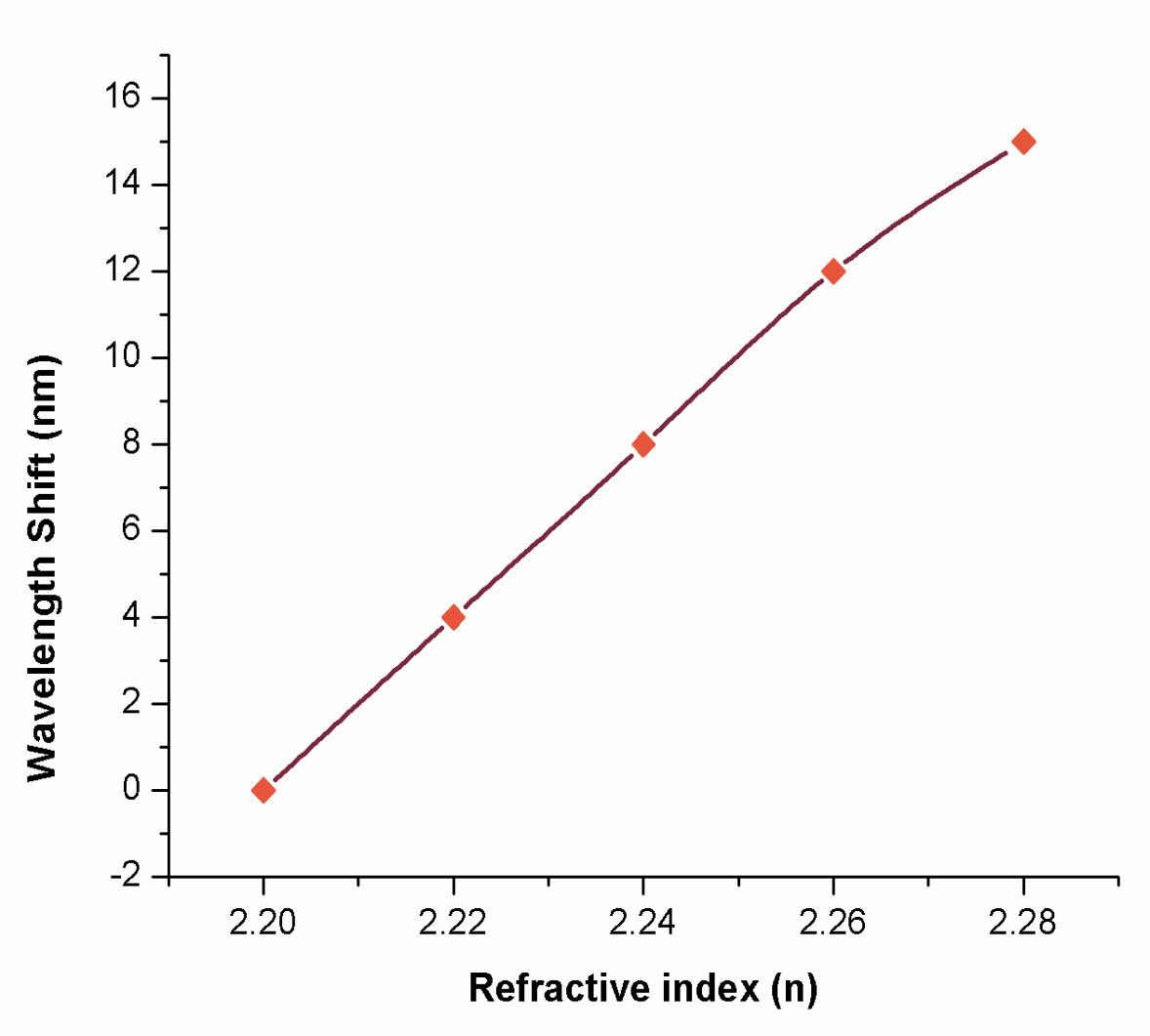

Figure 6.10 Plot between the shifts in the center resonant wavelength versus refractive index of different samples in case of circular ring structure.

These figures are plotted by considering the refractive index change of both coupling rods and inner ring rods according to the sample. There is almost a linear relation observed between wavelength shift and refractive index in the case of square ring structure while the relationship in the case of circular ring structure is little deviated from linearity. The change in refractive index of the sample can be derived by analyzing the wavelength shift of the center of the resonant peaks.

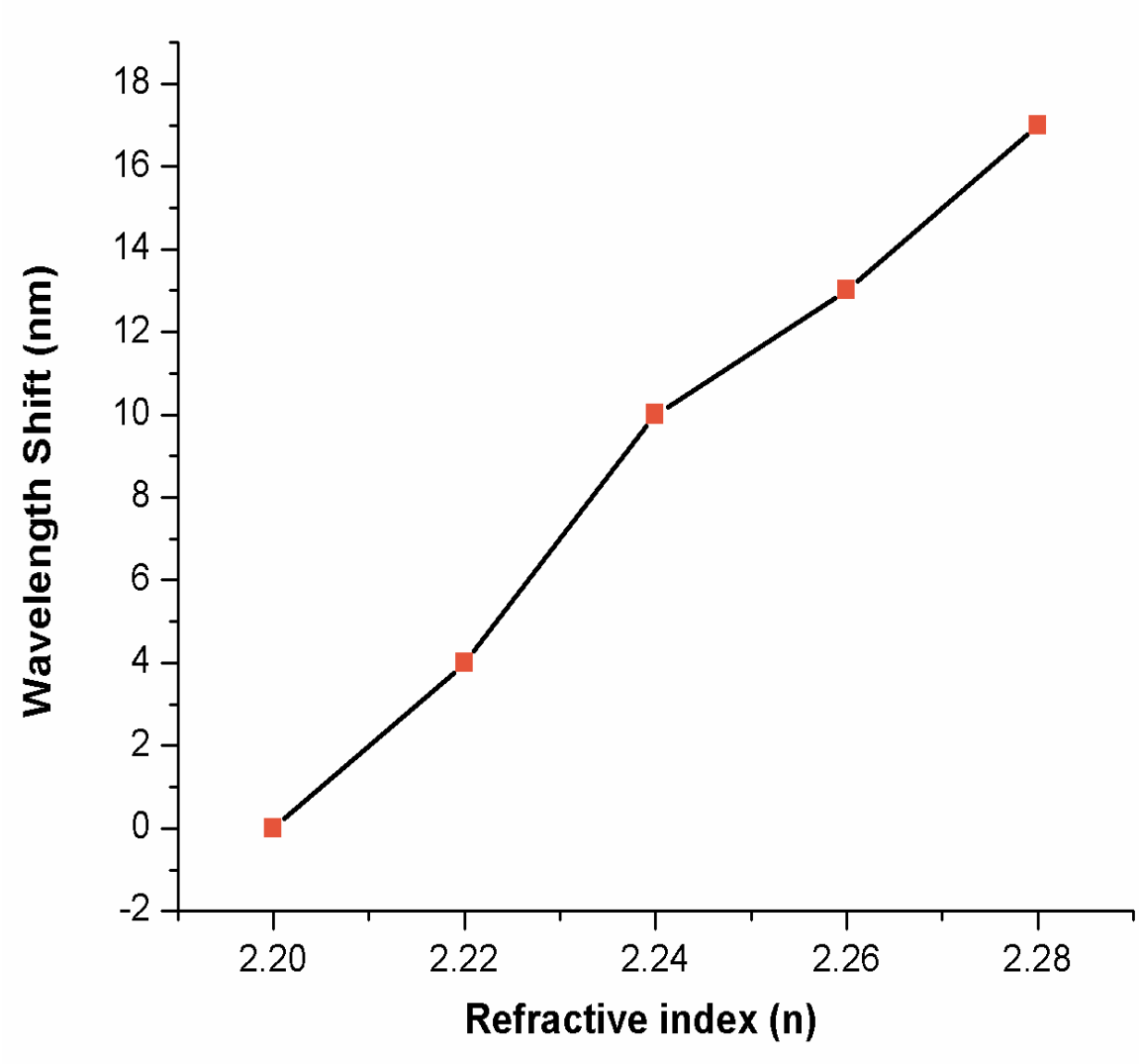

Figure 6.11 Plot between the shifts in the center resonant wavelength versus refractive index of different samples in case of square ring structure.

In addition to, PCRR containing 4 big rods as part of the ring cavity is also simulated for its output sensing characteristics. The 4 big rods in the cavity were then converted to elliptical shape and again the output sensing characteristics were studied. The refractive index of the PC rods is chosen to be 4.15 whereas the radius of the PC rods is made equal to 0.165 µm. Lattice constant, which is the distance between any two adjacent PC rods is fixed for band-gap calculation at 0.615 µm value. The input electromagnetic (EM) wave source is Gaussian in nature having a peak output at 1.55 µm. Performing 4 simulations by varying linearly the refractive index of the big rods from 3.1 to 3.7 in steps of 0.2, 4 resonance peaks are produced at the output for the case of structure as shown in Figure 6.12.

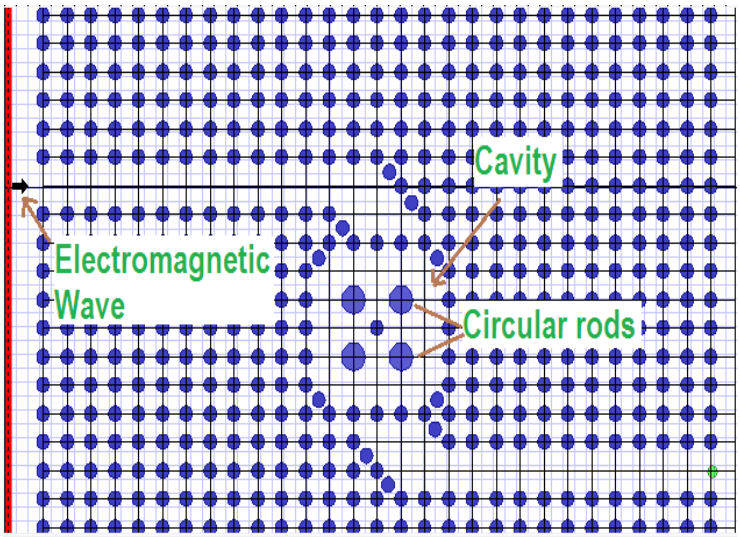

Figure 6.12 Layout of the PCRR with 4 big circular rods in the cavity.

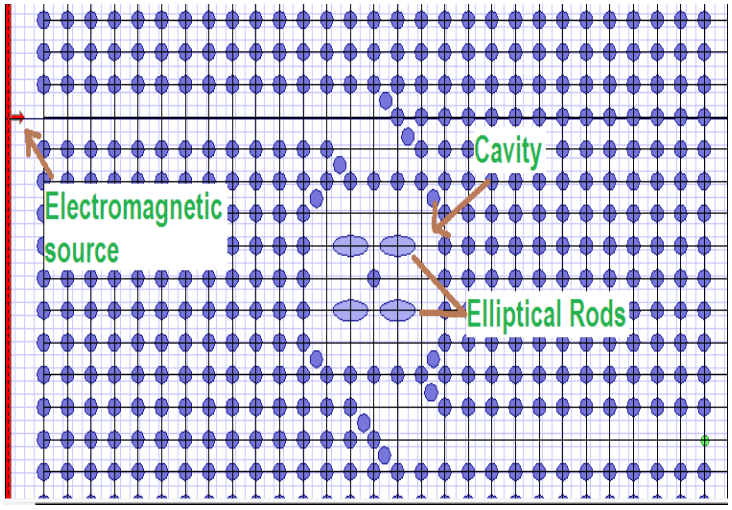

Figure 6.13 Layout of the PCRR with 4 big elliptical rods in the cavity.

Now the PCRR structure containing 4 elliptical rods as shown in Figure 6.13 is considered and simulations are performed exactly in the same manner as that for the previous structure. 4 resonant peaks are output in this case also. The output peaks of the both types of structure show that the peaks are shifting linearly in the increasing direction of wavelength as the refractive index of the 4 rods is increased from 3.1 to 3.7 as depicted in Figures 6.14 and 6.15 for circular and elliptical rods respectively.

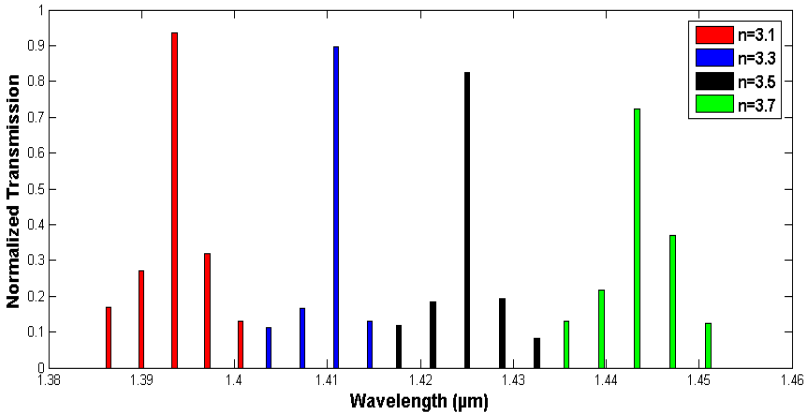

Figure 6.14 Output resonant peaks in case of big circular rods based PCRR.

.

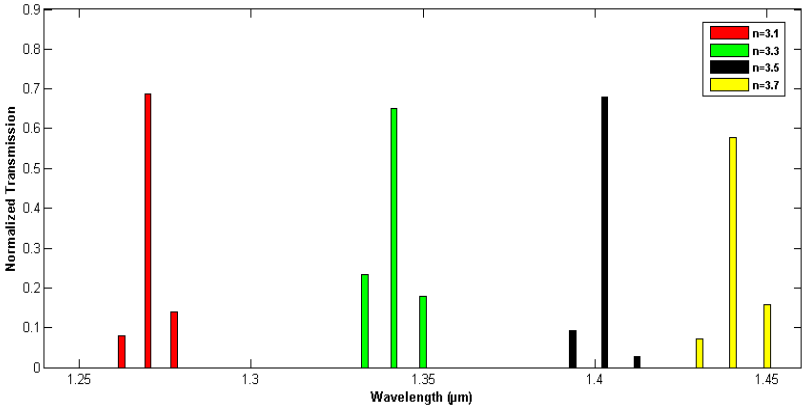

Figure 6.15 Output resonant peaks in case of big elliptical rods based PCRR.

The structure containing 4 big circular rods has a total shift of 0.05 μm wavelength between the first and last peaks whereas in the case of the structure with 4 big elliptical rods the total shift between the peaks has extended to about 0.16 μm wavelength. But at the same time the normalized power of the peaks in case of elliptical rods has decreased to about 65 percent as average of 4 peaks. Thus, on the basis of total shift between the resonant peaks which is directly proportional to sensitivity we can say that by employing elliptical rods we achieve more sensitivity as compared to the big circular rods.

6.4 CONCLUSION

Two types of photonic crystal ring resonators have been proposed for bio-chemical sensing based on square shape and circular shape of inner rings. The transmission characteristics of both types of ring resonators is studied by varying the refractive index of coupling rods, inner ring rods and both the coupling as well as inner ring rods at a time. The major difference between the output resonant peaks of square ring and circular ring structure is, the first peak of the circular ring structure is shifted in the right direction on the wavelength

scale as compared to that of square ring structure. The output resonant peaks extracted by varying the refractive index of inner ring rods only show a high sensitivity as compared to the peaks obtained by varying the refractive index of coupling rods or combination of coupling and inner ring rods. The average shift in the output resonant peaks for the square ring structure and circular ring structure comes out to be 2.75 nm and 3.5 nm respectively, on the wavelength scale for each 0.02 change in refractive index considered of inner ring rods alone. Thus we can deduce that both the square and circular ring photonic crystal resonators can act as real time bio-chemical sensors when the sample to be sensed are applied only on the inner ring for achieving high sensitivity. Nano photonic device based on our ring resonator structure can act as a potential candidate to serve in industrial or research sector which is working in the field of medicines, food testing, defence etc.